



## **Design and starting study of the adjustable inward turning inlet at Ma1.5~7**

*Liu Fuzhou<sup>1</sup>, Yuan Huacheng<sup>2</sup>, Zhou Keyu<sup>3</sup>, Zhou Zhenggu<sup>4</sup>*

### **Abstract**

Aiming at the challenges of the strong three-dimensional feature and difficulty in variable geometry for inward turning inlet, a variable-geometry design method combining inward turning and secondary shock wave compression is proposed. The start ability of the variable-geometry inward turning inlet is studied by numerical simulation, and the reason for reducing the start Mach number is analyzed. The results show that the Mach number range of the inlet start at the fixed-geometry state is broadened from  $Ma=3.5\sim 7$  to  $Ma=3\sim 7$ , compared to the original inward turning inlet. Besides, the variable-geometry method of rotating the secondary compression surface enables the inward turning inlet to operate with the start state at  $Ma=1.5\sim 2.5$ . Combined with the analysis of the isentropic criterion, it is found that the variable-geometry inward turning inlet proposed in this paper mainly improves the start capability by reducing both the mass flow coefficient and the total contraction ratio, thus realizing the inlet start at  $Ma=1.5\sim 7$ .

**Keywords:** *Inward turning inlet, Inlet start, Variable geometry, TBCC.*

### **Nomenclature**

$A_c$  - Area of the capture

$A_t$  - Area of the throat

CR - Total contraction ratio

$\theta_1$  - Rotation angle of the secondary  
compression surface

$\varphi$  - Mass flow coefficient

$\sigma_t$  - Total pressure recovery coefficient of the  
throat

Ma - Mach number of freestream

$Ma_t$  - Mach number of the throat

### **1. Introduction**

With the development of aerospace technology, horizontal takeoff/landing and reusable air-breathing hypersonic flight has gradually become a research hotspot [1]. To achieve wide-range flight from ground takeoff to hypersonic, the propulsion system is particularly critical. Currently, there are three types of power systems for hypersonic vehicles: turbojet, ramjet, and rocket engines. However, any single engine has a suitable operating range, making it difficult to meet the requirements for wide-range flight. Therefore, to achieve the aim of wide-speed range flight, combining multiple engines has become the optimal power solution for aircraft, such as Rocket-Based Combined-Cycle (RBCC) and Turbine-Based Combined-Cycle (TBCC) engines [2,3].

As the only windward component of combined cycle engines, the inlet plays the role of capturing and

<sup>1</sup> Nanjing University of Aeronautics and Astronautics, Yudao St. 29#, Qinhuai District, Nanjing, Jiangsu Province, People's Republic of China, liu\_fuzhou@nuaa.edu.cn

<sup>2</sup> Nanjing University of Aeronautics and Astronautics, Yudao St. 29#, Qinhuai District, Nanjing, Jiangsu Province, People's Republic of China, yuan\_public@126.com

<sup>3</sup> Nanjing University of Aeronautics and Astronautics, Yudao St. 29#, Qinhuai District, Nanjing, Jiangsu Province, People's Republic of China, 791843205@qq.com

<sup>4</sup> Nanjing University of Aeronautics and Astronautics, Yudao St. 29#, Qinhuai District, Nanjing, Jiangsu Province, People's Republic of China, zzgon@nuaa.edu.cn

compressing the incoming flow to meet the demands of different types of downstream engines, such as mass flow rate, total pressure recovery coefficient, and Mach number, and whether normal operating of the inlet affects the thrust level of the whole propulsion system. The inlet forms mainly include axisymmetric, two-dimensional, and inward turning inlets. As the flight Mach number extends to hypersonic speed, the inlet needs to compress the incoming flow to a certain Mach number to achieve high aerodynamic performance. In contrast, axisymmetric and two-dimensional inlets are designed as the form of multi-shock-wave compression [4], which leads to serious problems of shock wave boundary layer interaction in the flowpath, resulting in a decrease in compression efficiency. To alleviate the interaction between shock wave and boundary layer, some scholars have proposed the design concept of three-dimensional inward turning inlet [5] from the perspective of reducing shock wave compression. Compared to the axisymmetric and two-dimensional inlets, the inward turning inlet, due to the three-dimensional isentropic compression design, has higher capabilities of mass flow capturing and compression at hypersonic flight [6].

For wide-range operating inlets, to achieve excellent aerodynamic performance at hypersonic speeds, the design point of the inlet is generally greater than Mach number 5. However, when accelerating from low supersonic to high supersonic speeds, the inlet faces severe problems of inlet start [7,8], leading to a sharp decline in the thrust of the propulsion system. Taking a conventional turbofan engine as an example, the thrust can be decreased by approximately 1.25% for every 1.0% decline in the total pressure recovery coefficient of the inlet [9]. Therefore, to broaden the operating Mach number range of the inlet start as much as possible is the primary goal when designing a wide-range inlet, which requires the inlet to have the ability of variable geometry and adjustment [10]. For axisymmetric and two-dimensional inlets, the compression surface is regular and the adjusting geometry is relatively easy to implement. Common variable-geometry measures for axisymmetric inlets mainly involve moving the center cone and cowl [11-13], while two-dimensional inlets typically use rotating compression surfaces to adjust the inlet start [14,15]. However, when designing an internal turning inlet, the method of the inviscid characteristic line is generally adopted to calculate the reference flowfield [16,17], and the streamline tracking technique is employed to generate the compression surface of inward turning inlet [18]. As a result, the surface of inward turning inlet has the strong three-dimensional characteristic, making it more challenging to implement variable geometry. Presently, most variable-geometry measures of inward turning inlet in combined cycle engine schemes adopt the measure of rotating compression surface directly [19-21]. Although the original three-dimensional surface and isentropic compression characteristics of inward turning inlet are maintained at hypersonic speed, the issues of surface discontinuity and expansion corners during variable geometry are not considered. Therefore, how to keep the three-dimensional compression characteristics of the inward turning inlet during variable geometry is crucial for its application in wide-speed flight.

This paper proposed a design method for variable-geometry inward turning inlet. On the basis of maintaining the compression surface of the inward turning inlet, a secondary shock wave is introduced so that the compression efficiency of airflow is further improved at the high Mach number. When the inlet is in the unstart state at low Mach numbers, the secondary compression surface is adjusted to widen the operating range of the inlet start. Meanwhile, the three-dimensional compression characteristic of the inward turning is remained. And the start capability of the variable-geometry inward turning inlet was studied, aiming to widen the Mach number range of the inlet start to  $Ma=1.5\sim7$ .

## 2. Methodology

### 2.1. Design of the three-dimensional variable-geometry inward turning inlet

In this paper, a reference flowfield with an arctangent Mach number distribution is adopted, and the three-dimensional rectangle inward turning inlet is obtained through streamline tracking, as Fig. 1. The design Mach number is  $Ma=6$ , and the reference flowfield is internally conical, consisting of an initial three-dimensional curved cone shock wave, a reflected shock wave and the isentropic compression region between them. The rectangular entrance is projected onto the initial curved shock wave surface, forming the leading edge of the inward turning inlet. Starting from the leading edge, the technique of streamline tracking is used to form the compression surface. Since the streamlines in the reference flowfield show the inward contraction shape, the compression surface of the inward turning inlet has a strong three-dimensional characteristic.

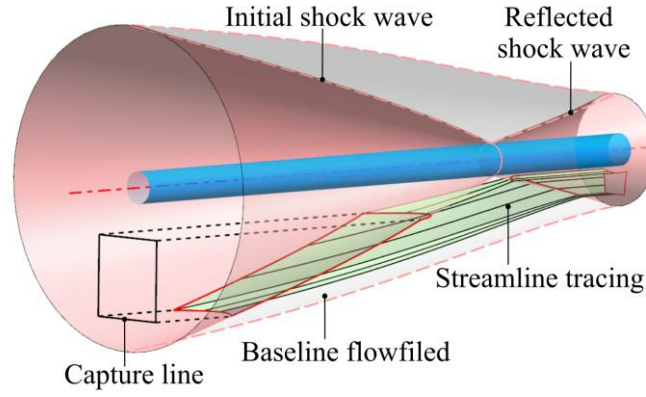


Fig 1. Reference flowfield and inward turning inlet

To maintain the three-dimensional isentropic compression characteristic of the inward turning inlet as much as possible, learning from the multi-shock-wave design methods of two-dimensional and axisymmetric inlets, a design method for the inward turning inlet with inward turning and shock wave compression is proposed, as Fig. 2. The design concept is as follows: based on the external compression section of the inward turning inlet, a secondary oblique shock wave is designed such that the initial shock wave generated by the initial angle  $\alpha_0$  and the secondary oblique shock wave generated by the angle  $\alpha_1$  are hitting on cowl lip on the symmetry plane, as Fig. 2(a). The compression surface after the secondary shock wave is designed based on Bezier curves. The specific steps are as follows: firstly, on the premise of keeping the captured leading edge of the inward turning inlet, the compression angle  $\alpha_1$  and initial location of secondary compression are determined by the oblique shock wave formula. Secondly, the truncation position of the sidewall can be gained according to the beginning position of the secondary compression and the cowl leading edge, so the truncation lines of secondary compression entrance are obtained. Finally, the compression surfaces between the secondary compression entrance and throat are designed by the cubic Bezier curves. The cowl lip angle  $\alpha_2$  on the symmetry plane can be adjusted to weaken the intensity of the cowl shock wave and avoid the flow separation. The design rule for the direction angles of the secondary compression entrance is that the angles of the leading edge of the compression surface and cowl adopt the linear variation law from the symmetry plane to the sidewall ( $\alpha_1$  to  $\alpha_{11}$ ,  $\alpha_2$  to  $\alpha_{12}$ ). Besides, the projection component of the sidewall angle  $\alpha_{11}$  on the symmetry plane is the same as the angle  $\alpha_1$  and the direction angles of the sidewall line are tangent to the original inward turning inlet, ensuring a smooth connection between the secondary compression surface and initial surface on the sidewall. The throat is designed as a rectangle with the same area as the original inward turning inlet, maintaining a total contraction ratio of  $CR=5$ . Finally, a fixed-geometry inward turning inlet with the characteristics of both inward turning and shock wave compression (ITSWC) is as Fig. 2(b).

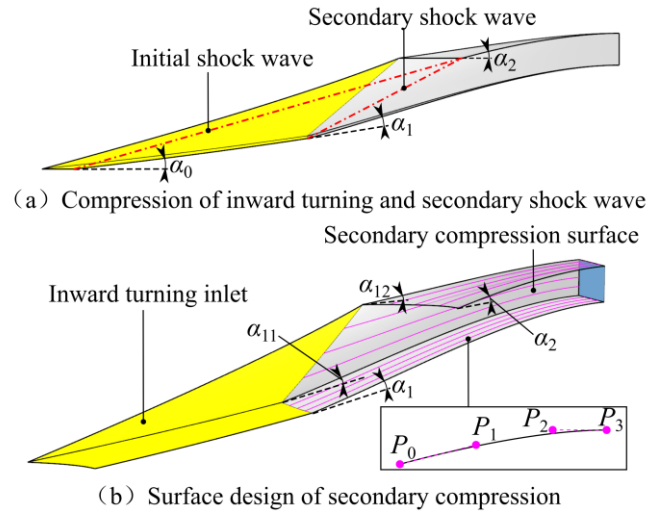


Fig 2. Design diagram of inward turning and shock wave compression inlet

The Bezier curve equations are as follows:

$$C(u) = \sum_{i=0}^n B_{i,n}(u)P_i \quad 0 \leq u \leq 1 \quad (1)$$

$$B_{i,n}(u) = \frac{n!}{i!(n-i)!} u^i (1-u)^{n-i} \quad (2)$$

Among them,  $P_i$  is the control point of curve,  $n$  represents the degree and  $n=3$  in this paper.

Based on the fixed-geometry ITSWC inlet, the variable-geometry ITSWC inlet is designed for the TBCC combined cycle engine, as Fig. 3. The variable-geometry measure adopts the rotating secondary compression surface to expand the throat area and reduce the total contraction ratio. Due to the spanwise contraction characteristic of the secondary compression, the envelope surface of the sidewall edge of the secondary compression sweeping is used as the sidewall surface during variable geometry, ensuring the airflow sealing of the sidewall. After the throat, it is divided into the ramjet, turbine, and bypass flowpaths. The mode transition is designed as a parallelogram mechanism to close or open the ramjet and turbine flowpaths. The advantages of variable-geometry ITSWC inlet are as follows: at high Mach number, the inlet has the characteristics of both three-dimensional inward turning compression and secondary shock wave compression, and the airflow is further compressed on the basis of the inward turning inlet to improve the compression efficiency. At low Mach number, the inward turning inlet can be adjusted from the unstart to start by rotating the secondary compression surface with angle  $\theta_1$ , while maintaining the three-dimensional compression characteristics of the inward turning inlet and avoiding the expansion corner.

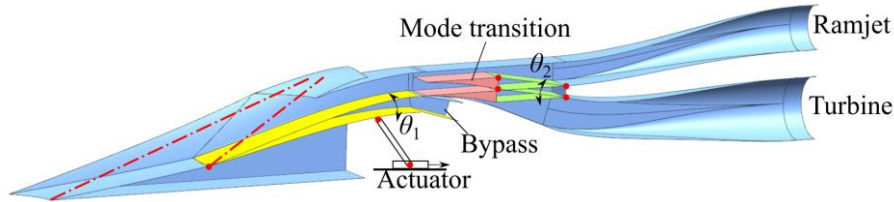


Fig 3. Variable-geometry ITSWC inlet

## 2.2. Numerical simulation methods

In this paper, numerical simulation methods are used to carry out research, and the wind tunnel experimental data of the variable-geometry inward turning inlet completed in the earlier stage are used to verify the reliability. The test model is as Fig. 4(a), the entrance shape is rectangular and the variable-geometry method is achieved by rotating the secondary compression surface. The grid system is as Fig. 4(b), adopting the structured grid, and nodes near the wall and airflow turning are refined especially. The steady flow is calculated by compressible Reynolds-averaged Navier–Stokes equations, spatially discretized by the Roe-FDS difference scheme. The air is regarded as an ideal gas and its viscosity employs the Sutherland formula. Besides, to select an appropriate turbulence model for simulating the flow of the inward turning inlet, the differences between the SA,  $k-\omega$  SST, and  $k-\epsilon$  RNG turbulence models and experimental results are compared.

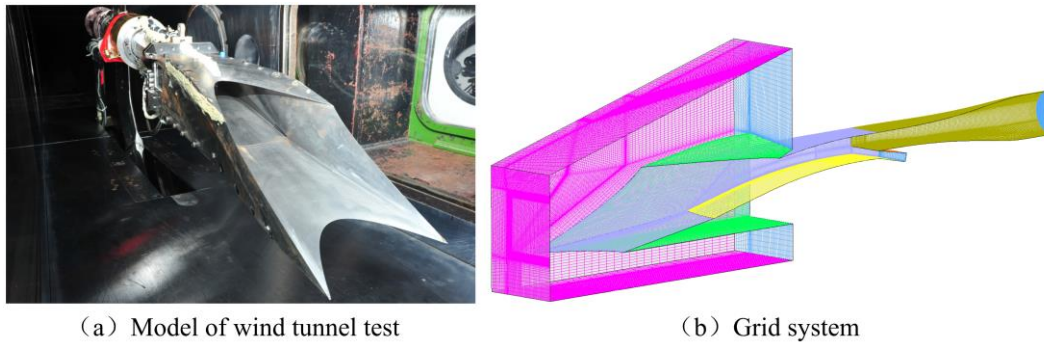


Fig 4. Model of wind tunnel test and grid system of the inward turning inlet

Fig. 5 shows the static pressure distribution curves along the wall of the numerical simulation and experiment, and the airflow speed of the nozzle outlet is  $Ma=4$  with total pressure of 0.63 MPa and total temperature of 288 K. It can be seen that the numerical simulation results of the three turbulence models coincide with the experimental data before the throat. However, there exists the structure of



the shock train in the diffuser, which leads to deviations in the pressure curve between the numerical simulation and the wind tunnel test, and the result of the SA turbulence model is relatively closer to experimental data. Therefore, the SA turbulence model is adopted in this paper.

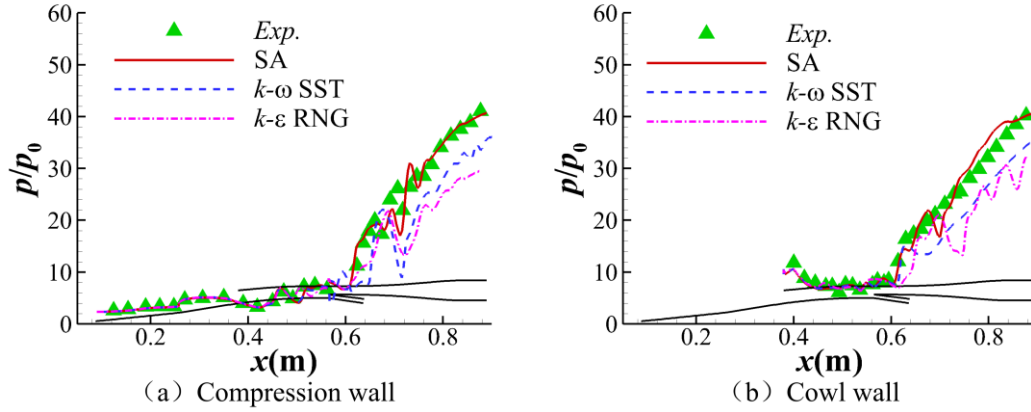


Fig 5. Static pressure distribution curves along the wall of the inward turning inlet

### 3. Results and Discussion

#### 3.1. Start characteristics of fixed-geometry inlet

At the design point  $Ma=6$ , the Mach number distribution contour of the ITSWC inlet is as Fig. 6(a). It can be seen that the initial shock wave and the secondary shock wave are hitting on cowl lip on the symmetry plane, verifying the inlet design method with inward turning and shock wave compression. In addition, the initial shock wave shows the shape of three-dimensional curved shock wave and is closely attached to the leading edge of the inlet, and the secondary shock wave presents the shape of planar oblique shock wave. Besides, the secondary shock wave enters the cowl lip on the spanwise slices because of the V-shape of cowl lip, but there is no flow separation due to the relatively weak intensity of the second shock wave. Compared to the flowfield of the baseline inward turning inlet, as Fig. 6(b), the three-dimensional isentropic compression region behind the initial shock wave of the ITSWC inlet reduces, while the compression ratio of shock wave increases.

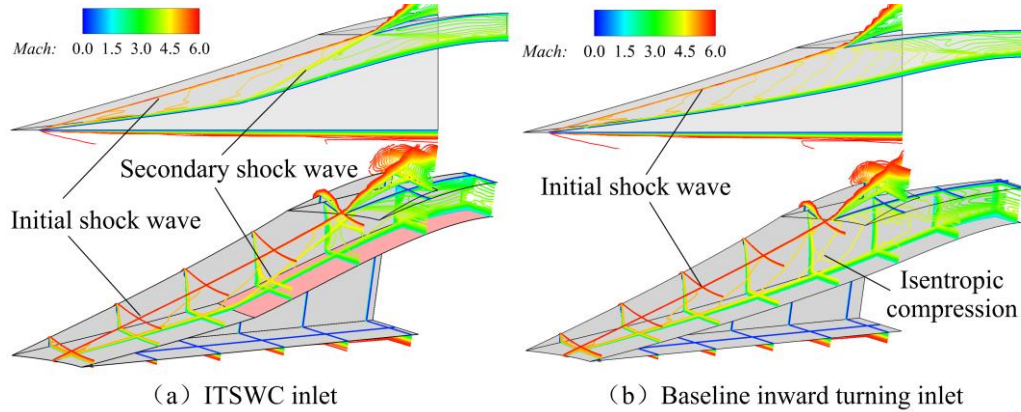


Fig 6. Mach number contour of ITSWC inlet and baseline inward turning inlet at  $Ma=6$

At the off-design point, the initial shock wave angle increases as the flight Mach number decreases and the supersonic overflow window appears in front of the cowl, as Fig. 7(a). Among that, the capturing streamline  $S_0'$  originates from the leading edge of the cowl, corresponding to the mass flow of the inlet. Compared to the baseline inward turning inlet, the capturing streamline  $S_0$  of the ITSWC inlet is lower due to introducing the secondary oblique shock wave, which means the larger supersonic overflow window and results in a decrease in mass flow coefficient, as Fig. 7(b).

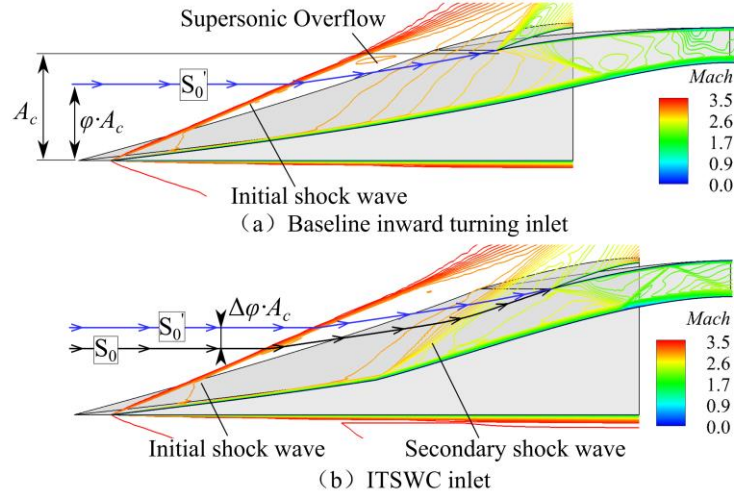


Fig 7. Mach number contour of ITSWC inlet and baseline inward turning inlet at  $Ma=3.5$

As the flight Mach number decreases, the difference in mass flow coefficient  $\Delta\varphi$  between the baseline inward turning inlet and ITSWC inlet increases, as Fig. 8(a). Therefore, the mass flow coefficient of the ITSWC inlet is relatively smaller at low Mach numbers, which can make the inlet more likely to be in the start state under the same total contraction ratio. Additionally, compared to the baseline inward turning inlet, the total pressure recovery coefficient of throat drops because of the addition of the secondary shock wave, as Fig. 8(b). However, the minimum starting Mach number of the fixed-geometry ITSWC inlet is reduced from  $Ma=3.5$  to  $Ma=3$ , which reduces the difficulty of adjusting geometry for the inlet start.

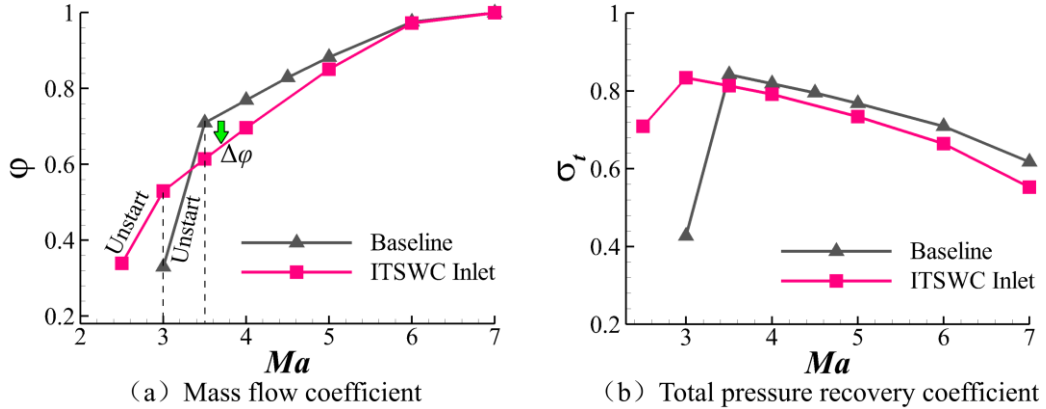


Fig 8. Performance comparison of ITSWC inlet and baseline inward turning inlet

### 3.2. Start characteristics of variable-geometry inlet

According to the isentropic criterion [7], the main factor affecting the inlet start is the total contraction ratio. Thus, to achieve the range of starting operation from  $Ma=1.5$  to  $Ma=6+$ , the inlet must have the ability to adjust the total contraction ratio over a wide range, as Fig. 9(a). Based on the scheme of variable-geometry ITSWC inlet, the relationship between the total contraction ratio and the rotation angle of the secondary compression surface is established, as Fig. 9(b). It can be seen that the throat area increases as the rotation angle  $\theta_1$  increases, and the total contraction ratio exhibits a decreasing trend of cosine. Besides, the total contraction ratio CR of the ITSWC inlet varies from 2 to 5 by adjusting the secondary compression surface, providing great potential for decreasing the minimum starting Mach number. Since the start range of the fixed-geometry ITSWC inlet is  $Ma=3\sim7$ , the variable geometry characteristics of the ITSWC inlet for  $Ma=1.5\sim2.5$  are studied to achieve the goal of wide-speed flight. During the research, the ramjet flowpath is closed by the splitter wedge of mode transition.

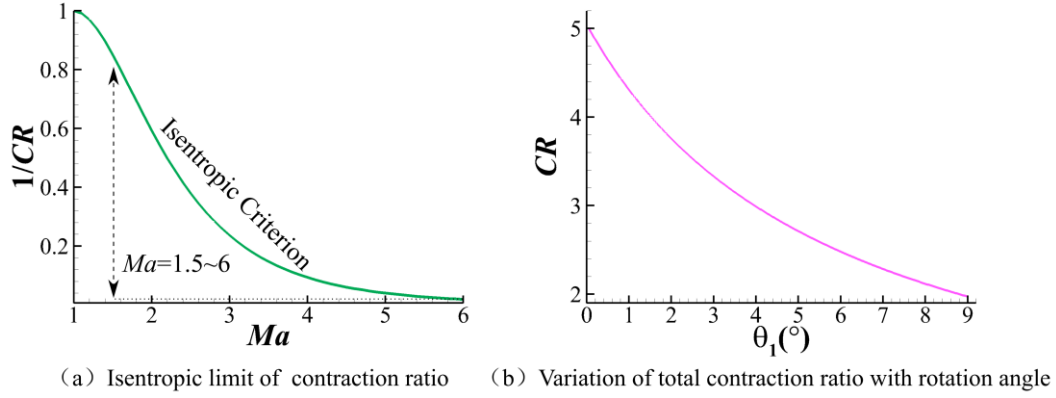
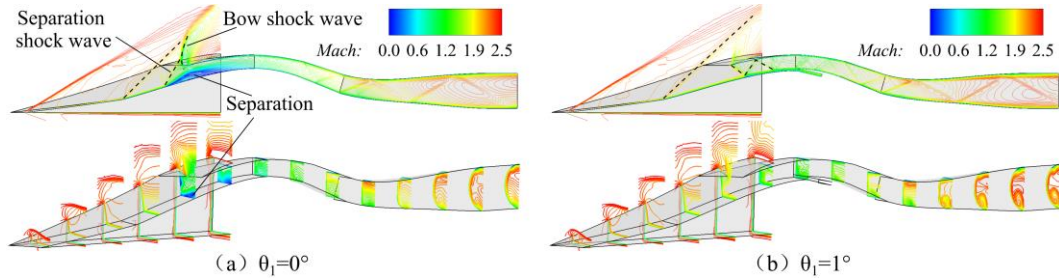


Fig 9. Start analysis of the wide-range inlet

Due to the total contraction ratio  $CR=5$  of the fixed-geometry ITSWC inlet, airflow choking occurs in the throat at  $Ma=2.5$ , leading to a bow shock wave in front of the lip, and the inlet is in the unstart state, as Fig. 10(a). The root of the bow shock wave induces a three-dimensional separation bubble, which causes a separation shock wave and the subsonic flow of the internal contraction section. As the rotation angle  $\theta_1$  of the secondary compression surface increases, the total contraction ratio of the ITSWC inlet decreases. At  $\theta_1=1^\circ$ , the bow shock wave and separation bubble in front of the cowl lip disappear. Besides, a reflected shock wave system is established and the core airflow is all supersonic in the internal compression section, indicating the inlet start, as Fig. 10(b). At this time, the total contraction ratio of the inlet is  $CR=4.30$  and the bypass flowpath is opened.


 Fig 10. Mach number contour of variable-geometry inlet at different rotation angle when  $Ma=2.5$ 

At  $Ma=2$ , the bow shock wave at the unstart state becomes weaker due to the decrease in flight Mach number, resulting in a smaller separation at the shock wave root so that it looks like a "λ-shape" shock wave, as Fig. 11(a). As the rotation angle of the secondary compression surface increases to  $\theta_1=3^\circ$ , corresponding to the total contraction ratio  $CR=3.30$ , the inlet is in the start state, as Fig. 11(b). At  $Ma=1.5$ , the "λ-shape" shock wave converts to a bow shock wave when the inlet is in the unstart state, as Fig. 12(a). According to the isentropic criterion, a smaller total contraction ratio is required for the inlet start, which corresponds to a larger rotation angle of the secondary compression surface. When the rotation angle increases to  $\theta_1=6^\circ$ , corresponding to the total contraction ratio decreasing to  $CR=2.48$ , the bow shock wave in front of the cow lip disappears and the inlet is in the start state, as Fig. 12(b). Meanwhile, the secondary compression surface is tangent to the initial inward turning inlet and the secondary shock wave disappears, leaving the ITSWC inlet with only the characteristic of three-dimensional inward turning compression. Additionally, since the internal contraction section is expanding in the height direction, there are no reflected shock waves. As a result, by rotating the secondary compression surface to decrease the total contraction ratio, the minimum starting Mach number of the inward turning inlet can be reduced to  $Ma=1.5$  while maintaining its three-dimensional compression characteristic, demonstrating the feasibility of the variable-geometry design method.

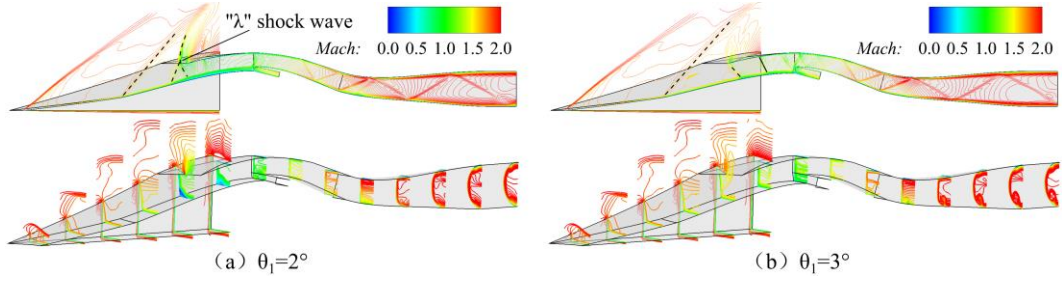
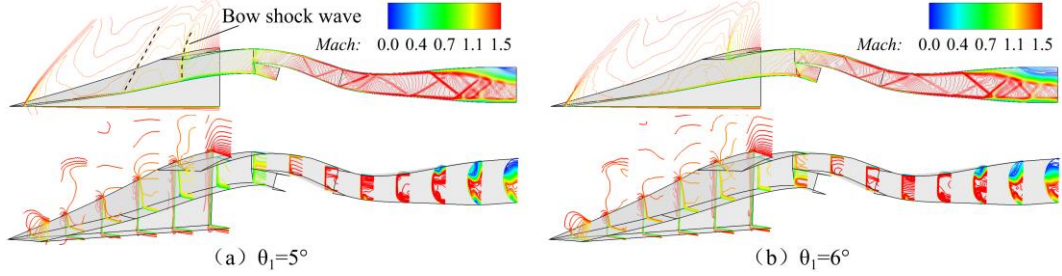
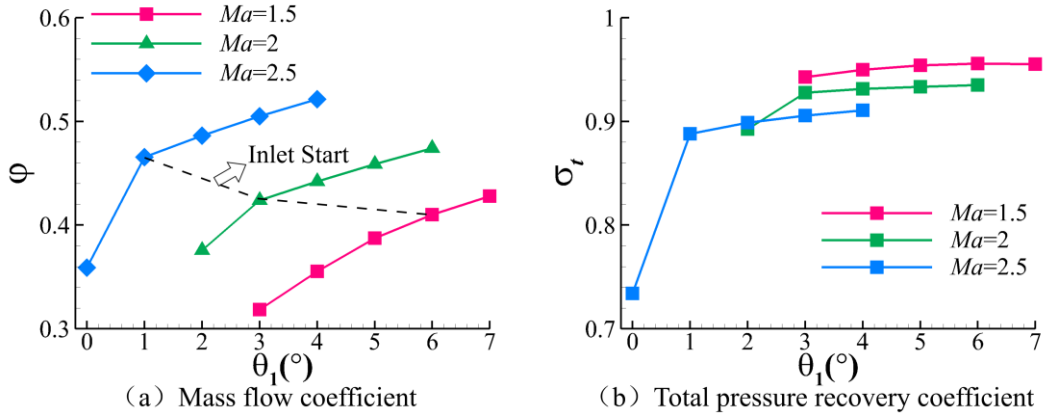

 Fig 11. Mach number contour of variable-geometry inlet at different rotation angle when  $Ma=2$ 

 Fig 12. Mach number contour of variable-geometry inlet at different rotation angle when  $Ma=1.5$ 

Fig. 13 shows the variation curve of throat performance parameters with the rotation angle of the secondary compression surface at  $Ma=1.5\sim 2.5$ . It can be seen that the mass flow coefficient and total pressure recovery coefficient drop sharply when the inlet is in the unstart state, which is induced by the bow shock wave in front of the cowl lip. After the inlet is in the start state, the angle of the secondary shock wave decreases as the rotation angle  $\theta_1$  increases so that the mass flow coefficient almost shows a linear increasing trend, as Fig. 13(a). At the same time, the intensity of the secondary shock wave decreases as the rotation angle  $\theta_1$  increases, leading to a rise in the total pressure recovery coefficient, as Fig. 13(b). However, the increase in total pressure recovery coefficient is not significant due to the small loss of the secondary shock wave under different rotation angles  $\theta_1$ .


 Fig 13. Variation of the throat performance with the rotation angle at  $Ma=1.5\sim 2.5$ 

### 3.3. Start analysis of the adjustable inward turning inlet

Since the flow behind the initial shock wave of the inward turning inlet is close to the three-dimensional isentropic compression flow, as Fig. 14, the isentropic criterion is used for start analysis. The definition of the isentropic limit is the area contraction ratio that will produce sonic flow at the throat after isentropic compression. Note that the definition object of the isentropic limit is for internal compression inlet or the internal compression section of the inlet. Furthermore, it only takes into account the area contraction ratio, neglecting the impact of the mass flow coefficient and the total pressure loss.



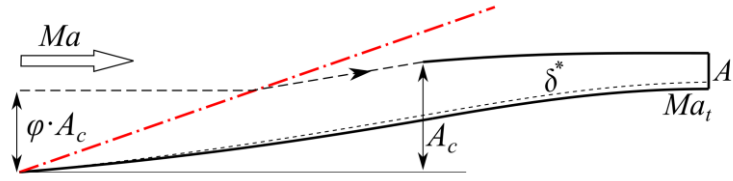


Fig 14. Diagram of flow in front of throat

Thus, the theoretical start boundary of the inward turning inlet, considering the influence of the mass flow coefficient and the total pressure recovery coefficient, can be calculated by Eq. 3:

$$CR = \frac{A_c}{A_t} = \frac{\sigma_t}{\phi q(Ma)} q(Ma_t) \quad (3)$$

It can be seen from Eq. 3 that the factors affecting the minimum start Mach number are the total contraction ratio CR, the mass flow coefficient  $\phi$  and the total pressure recovery coefficient of the throat  $\sigma_t$ . Fig. 15 shows the theoretical start boundary curves of different  $\sigma_t/\phi$  by Eq. 3 and the right side of the curve represents the region of the inlet start. And  $\sigma_t/\phi=1$  represents the traditional isentropic limit and the theoretical boundaries of  $\sigma_t/\phi=2.32$ , 2.16 and 1.89 are respectively gained according to the numerical simulation result of start boundary at  $Ma=1.5$ , 2 and 2.5, note that  $Ma_t=1$ . It is found that the start boundary considering the mass flow coefficient and the total pressure recovery coefficient is much lower than the classical isentropic criterion. According to the numerical simulation result, the total contraction ratios of the start boundary at  $Ma=1.5$ , 2 and 2.5 by rotating secondary compression surface are  $CR=2.48$ , 3.30 and 4.30 respectively, which are located just to the right of the theory boundary curve and indicate the correct of the theoretical start boundary for the inward turning inlet. However, there is a small deviation of the start boundary between the numerical simulation and the theory. The reasons are as follows: firstly, the Mach number of the throat is greater than 1 when the inlet is in the start state under numerical simulation conditions. secondly, the influence of the boundary layer on the total contraction ratio needs to be considered. In general, Eq. 3 can be used to guide the design and analysis of variable-geometry inlet.

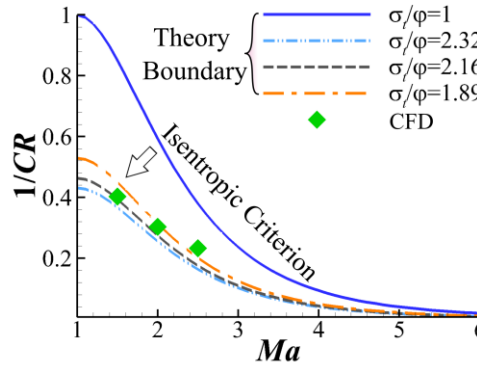


Fig 15. Start boundary of the variable-geometry ITSWC inlet

According to Eq. 3, the secondary shock wave increases the supersonic overflow and reduces the captured mass flow coefficient under the same total contraction ratio  $CR=5$ , which is the reason that the minimum start Mach number of the fixed-geometry ITSWC inlet decreases from  $Ma=3.5$  to  $Ma=3$ . During the progress of variable geometry, although the captured mass flow coefficient of the ITSWC inlet increases as the rotation angle decreases, the secondary shock wave still makes it smaller than that of the baseline inward turning inlet, which is beneficial for the inlet start. At the same time, the total contraction ratio decreases from  $CR=5$  to  $CR=2.48$  by rotating the secondary compression surface, which reduces the minimum starting Mach number of the ITSWC inlet to  $Ma=1.5$  and achieves the variable-geometry design goal of starting operation at  $Ma=1.5\sim 7$ . According to the shock wave theory, the total pressure recovery coefficient behind the normal shock wave at  $Ma<1.5$  is higher than 0.9. Therefore, the variable-geometry design method of inward turning and shock wave compression has the potential to achieve the wide-range flight at  $Ma=0\sim 7$ .

#### 4. Conclusions

In this paper, a variable-geometry inlet design method for inward turning and shock wave compression is proposed, and its starting and flow characteristics are studied. The conclusions are as follows:

- (1) The second oblique shock wave weakens the high mass flow capture characteristic of the inward turning inlet at low Mach number, reducing the minimum start Mach number of the fixed-geometry inlet from  $Ma=3.5$  to  $Ma=3$ , demonstrating excellent start performance of fixed-geometry inlet design.
- (2) A wide range of total contraction ratios can be achieved by rotating the secondary compression surface. At  $Ma=1.5$ , 2 and 2.5, the total contraction ratios are 2.48, 3.30 and 4.30 respectively when the inlet is in the start state, corresponding to the secondary compression surface respectively rotating  $6^\circ$ ,  $3^\circ$  and  $1^\circ$ .
- (3) It is found that the factors affecting the inlet start are the total contraction ratio, mass flow coefficient and total pressure recovery coefficient of the throat by the improved formula of isentropic limit. The variable-geometry inward turning inlet in this paper mainly improves the start capability by reducing both the mass flow coefficient and the total contraction ratio, enabling the inward turning inlet to operate with the start state at  $Ma=1.5\sim 7$ .

The variable-geometry design method proposed in this paper keeps the high efficiency compression characteristic of the inward turning inlet and possesses the potential to adjust the inlet start, providing reference and inspiration for the wide-range air-breathing flight at  $Ma=0\sim 7$ .

#### Acknowledgments

This study was co-supported by the National Natural Science Foundation of China (12302299), the Science Center for Gas Turbine Project (P2022-B-I-004-001), the Science and Technology on Scramjet Laboratory (2023-JCJQ-LB-018-007).

#### References

1. McClinton, C.R., Rausch, V.L., Shaw, R.J., Metha, U., Naftel, C.: Hyper-X: Foundation for future hypersonic launch vehicles. *Acta Astronautica* 57(2-8), 614-622 (2005).
2. Shi, L., Yang, Y.Y., Zhao, G.J., Liu, P.J., Zhao, D., Qin, F., Wei, X.G., He, G.Q.: Research and development on inlets for rocket based combined cycle engines. *Progress in aerospace and sciences* 117 (2020).  
<https://doi.org/10.1016/j.paerosci.2020.100639>
3. Snyder, L., Escher, D., DeFrancesco, R., Gutierrez, J., Buckwalter, D.: Turbine Based Combination Cycle (TBCC) Propulsion Subsystem Integration. In: 40th AIAA/ASME/SAE/ASEE Joint Propulsion Conference and Exhibit (2004).  
<https://doi.org/10.2514/6.2004-3649>
4. Zhang, Z.Z., Shi, L., Wang, Y.J., Qin, F., He, G.Q., Liu, P.J.: Numerical Investigations on RBCC Variable Inlet in  $Ma=2-6$ . In: 21st AIAA International Space Planes and Hypersonics Technologies Conference (2017).  
<https://doi.org/10.2514/6.2017-2431>
5. Mölder, S., Szpiro, E.J.: Busemann inlet for hypersonic speeds. *Journal of Spacecraft and Rockets* 3(8), 1303-1304 (1966).
6. You, Y.C.: An Overview of the Advantages and Concerns of Hypersonic Inward Turning Inlets. In: 17th AIAA International Space Planes and Hypersonic Systems and Technologies Conference (2011).  
<https://doi.org/10.2514/6.2011-2269>
7. Van Wie, D.M., Kwok, F.T., Walsh, R.F.: Starting characteristics of supersonic inlets. In: 32nd Joint Propulsion Conference and Exhibit (1996).  
<https://doi.org/10.2514/6.1996-2914>
8. Chang, J.T., Li, N., Xu, K.J., Bao, W., Yu, D.R.: Recent research progress on unstart mechanism, detection and control of hypersonic inlet. *Progress in Aerospace Sciences* 89, 1-22 (2017).

9. Liu, D.X.: Aeroengine Design Manual - Volume 7: Intake and exhaust devices. Beijing: Aviation Industry Press, pp. 4 (2004).
10. Wang, Z.Y., Yu, H., Zhang, Y., Tan, H.J., Jin, Y., Li, X.: Research progress on key issues of adjustable inlet system for aerospace vehicles. *Acta Aeronautica et Astronautica Sinica* 45, 529440 (2024).
11. Kojima, T., Tanatsugu, N., Sato, T., Kanda, M., Enomoto, Y.: Development study on axisymmetric air inlet for ATREX engine. In: 10th AIAA/NAL-NASDA-ISAS International Space Planes and Hypersonic Systems and Technologies Conference (2001).  
<https://doi.org/10.2514/6.2001-1895>
12. Colville, J., Lewis, M.: An Aerodynamic Redesign of the SR-71 Inlet with Applications to Turbine Based Combined Cycle Engines. In: 40th AIAA/ASME/SAE/ASEE Joint Propulsion Conference and Exhibit (2004).  
<https://doi.org/10.2514/6.2004-3481>
13. Colville, J., Starkey, R., Lewis, M.: Extending the Flight Mach Number of the SR-71 Inlet. In: AIAA/CIRA 13th International Space Planes and Hypersonics Systems and Technologies Conference (2005).  
<https://doi.org/10.2514/6.2005-3284>
14. Saunders, J.D., Stueber, T.J., Thomas, S.R., Suder, K.L., Weir, L.J., Sanders, B.W.: Testing of the NASA Hypersonics Project Combined Cycle Engine Large Scale Inlet Mode Transition Experiment (CCE LIMX). NASA/TM-2012-217217 (2012).
15. Yang, H., Ma, J., Man, Y.J., Zhu, S.M., Ling, W.H., Cao, X.B.: Numerical Simulation of Variable-Geometry Inlet for TRRE Combined Cycle Engine. In: 21st AIAA International Space Planes and Hypersonics Technologies Conference (2017).  
<https://doi.org/10.2514/6.2017-2437>
16. Billig, F.S., Jacobsen, L.S.: Comparison of Planar and Axisymmetric Flowpaths for Hydrogen Fueled. In: 39th AIAA/ASME/SAE/ASEE Joint Propulsion Conference and Exhibit (2003).  
<https://doi.org/10.2514/6.2003-4407>
17. Shi, C.G., Zhu, C.X., You, Y.C., Zhu, G.S.: Method of curved-shock characteristics with application to inverse design of supersonic flowfields. *Journal of Fluid Mechanics* 920 (2021).  
<https://doi.org/10.1017/jfm.2021.454>
18. Billig, F.S., Kothari, A.P.: Streamline Tracing: Technique for Designing Hypersonic Vehicles. *Journal of Propulsion and Power* 16(3), 465-471 (2000).
19. Walker, S., Tang, M., Morris, S., Mamplata, C.: Falcon HTV-3X - A Reusable Hypersonic Test Bed. In: 15th AIAA International Space Planes and Hypersonic Systems and Technologies Conference (2008).  
<https://doi.org/10.2514/6.2008-2544>
20. Zhu, C.X., Zhang, X., Kong, F., You, Y.C.: Design of a Three-Dimensional Hypersonic Inward-Turning Inlet with Tri-Ducts for Combined Cycle Engines. *International Journal of Aerospace Engineering* (2018).  
<https://doi.org/10.1155/2018/7459141>
21. Zuo, F.Y., Mölder, S.: Hypersonic wavecatcher intakes and variable-geometry turbine based combined cycle engines. *Progress in Aerospace Sciences* 106, 108-144 (2019).